pISSN 1598-2998, eISSN 2005-9256

https://doi.org/10.4143/crt.2020.704

Cancer Res Treat. 2021;53(1):162-171

Original Article

Spatial Distribution and Prognostic Implications of Tumor-Infiltrating FoxP3$^-$ CD4$^+$ T Cells in Biliary Tract Cancer

Hyung-Don Kim[1], **Jwa Hoon Kim**[1], **Yeon-Mi Ryu**[2], **Danbee Kim**[1], **Sunmin Lee**[1], **Jaehoon Shin**[3], **Seung-Mo Hong**[3], **Ki-Hun Kim**[4], **Dong-Hwan Jung**[4], **Gi Won Song**[4], **Dae Wook Hwang**[4], **Jae Hoon Lee**[4], **Ki Byung Song**[4], **Baek-Yeol Ryoo**[1], **Jae Ho Jeong**[1], **Kyu-pyo Kim**[1], **Sang-Yeob Kim**[2], **Changhoon Yoo**[1]

[1]Department of Oncology, Asan Medical Center, University of Ulsan College of Medicine, Seoul, [2]Asan Institute for Life Sciences, Asan Medical Center, Seoul, Departments of [3]Pathology and [4]Surgery, Asan Medical Center, University of Ulsan College of Medicine, Seoul, Korea

Purpose The clinical implications of tumor-infiltrating T cell subsets and their spatial distribution in biliary tract cancer (BTC) patients treated with gemcitabine plus cisplatin were investigated.

Materials and Methods A total of 52 BTC patients treated with palliative gemcitabine plus cisplatin were included. Multiplexed immunohistochemistry was performed on tumor tissues, and immune infiltrates were separately analyzed for the stroma, tumor margin, and tumor core.

Results The density of CD8$^+$ T cells, FoxP3$^-$ CD4$^+$ helper T cells, and FoxP3$^+$ CD4$^+$ regulatory T cells was significantly higher in the tumor margin than in the stroma and tumor core. The density of LAG3$^-$ or TIM3-expressing CD8$^+$ T cell and FoxP3$^-$ CD4$^+$ helper T cell infiltrates was also higher in the tumor margin. In extrahepatic cholangiocarcinoma, there was a higher density of T cell subsets in the tumor core and regulatory T cells in all regions. A high density of FoxP3$^-$ CD4$^+$ helper T cells in the tumor margin showed a trend toward better progression-free survival (PFS) (p=0.092) and significantly better overall survival (OS) (p=0.012). In multivariate analyses, a high density of FoxP3$^-$ CD4$^+$ helper T cells in the tumor margin was independently associated with favorable PFS and OS.

Conclusion The tumor margin is the major site for the active infiltration of T cell subsets with higher levels of LAG3 and TIM3 expression in BTC. The density of tumor margin-infiltrating FoxP3$^-$ CD4$^+$ helper T cells may be associated with clinical outcomes in BTC patients treated with gemcitabine plus cisplatin.

Key words Biliary tract cancer, Multiplexed immunohistochemistry, Tumor margin, CD4$^+$ helper T cells

Introduction

Biliary tract cancer (BTC) is an aggressive set of diseases including extrahepatic cholangiocarcinoma (EHCCA), intrahepatic cholangiocarcinoma (IHCCA), and gallbladder cancer (GBCA). Gemcitabine plus cisplatin (GemCis) is the current standard of care for patients with advanced BTC [1]; however, clinical outcomes remain considerably poor with a median survival of < 1 year in cases of unresectable disease. Recent advances in molecular classification and the development of targeted therapy including fibroblast growth factor receptor and isocitrate dehydrogenase 1 inhibitors may allow precision therapy; however, only a small proportion of BTC patients may benefit from this [2-4].

The efficacy of various immune checkpoint inhibitors (ICIs) has been investigated in patients with advanced BTC, which showed encouraging results with objective response rates of 5%-20% and durable responses in a chemotherapy-refractory setting [5-7]. However, a limited number of patients benefit from ICIs, highlighting the importance of characterizing the immune landscape in the tumor microenvironment (TME) of BTC [8]. Among the different immune subsets, T cell subsets such as cytotoxic CD8$^+$ T cells, helper CD4$^+$ T cells, and regulatory T cells are recognized as key components in anti-tumor immune responses [9-11]. Previous studies have examined the prognostic value of BTC-infiltrating T cells using conventional immunohistochemistry mainly in early-stage resectable diseases [12,13]. However, studies are rarely conducted for unresectable or metastatic diseases. As the immune landscape may affect the clinical outcomes of cancer patients in the context of systemic therapy [14-16], the immune profiles of patients with advanced BTC treated with systemic therapies should be investigated.

Spatial heterogeneity is one of the key features of the TME

Correspondence: Changhoon Yoo
Department of Oncology, Asan Medical Center, University of Ulsan College of Medicine, 88 Olympic-ro 43-gil, Songpa-gu, Seoul 05505, Korea
Tel: 82-2-3010-1727 Fax: 82-2-3010-6961 E-mail: yooc@amc.seoul.kr

Co-correspondence: Sang-Yeob Kim
Asan Institute for Life Sciences, Asan Medical Center, 88 Olympic-ro 43-gil, Songpa-gu, Seoul 05505, Korea
Tel: 82-2-3010-4139 E-mail: sykim3yk@amc.seoul.kr

Received July 14, 2020 **Accepted** August 28, 2020
Published Online August 31, 2020

*Hyung-Don Kim and Jwa Hoon Kim contributed equally to this work.

[17], and the composition and localization of immune infiltrates substantially vary depending on their dynamic interactions with tumor or stromal cells [18,19]. Notably, the spatial distribution of immune infiltrates in the TME has been reported to be associated with different clinical implications in patients who received systemic therapy [14,15]. However, little is known about the spatial heterogeneity of immune infiltrates and their clinical implications in BTC, especially in the context of systemic therapy.

In this study, we performed multiplexed immunohistochemistry (mIHC) to investigate the features of tumor-infiltrating T cell subsets in BTC patients treated with GemCis. We focused on their spatial distribution and associated clinical implications.

Materials and Methods

1. Study patients and GemCis therapy

The study patients were selected from a retrospective cohort of 740 patients with advanced BTC treated with GemCis as palliative therapy at Asan Medical Center (Seoul, Korea) (source population) [20]. Among 358 patients who underwent surgical resection, 60 patients were chosen for mIHC analyses, and 52 patients whose specimen passed quality control for mIHC were included in the study population (S1 Fig.). For all study patients, surgical specimens were used in the analysis of the spatial distribution of immune subsets.

Gemcitabine (1,000 mg/m^2 intravenously on days 1 and 8) and cisplatin (25 mg/m^2 intravenously on days 1 and 8) were administered every 3 weeks until disease progression or unacceptable adverse events occurred. The tumor response was evaluated every 8-12 weeks using computed tomography scans and graded by the Response Evaluation Criteria in Solid Tumors (RECIST) ver. 1.1.

2. mIHC

Optimized fluorescent mIHC was performed using tyramide signal amplification in the Leica Bond Rx Automated Stainer (Leica Biosystems, Newcastle, UK). Cells were stained with antibodies against CD4 (ab133616, Abcam, Cambridge, UK), CD8 (98941S, Cell Signaling Technology, Danvers, MA or MCA1817, Bio-Rad, Hercules, CA), FoxP3 (ab20034, Abcam), cytokeratin (NBP2-29429, Novus, Cambridge, UK), LAG3 (LS-C18692, LSBio, Seattle, WA), TIM3 (45208S, Cell Signaling Technology), granzyme B (262A-15, Cell Marque, Rocklin, CA), and CD45RO (ab23, Abcam), and the fluorescence signals were captured with the following fluorophores: Opal 480, Opal 520, Opal 570, Opal 620, Opal 690, and Opal 780. Multiplex-stained slides were obtained using the Vectra Polaris Quantitative Pathology Imaging System (Perkin Elmer, Boston, MA). We subdivided the tumor regions into the stroma, tumor margin, and tumor core. Regions of interest (ROIs) representing each subsection were carefully chosen by a pathologist specializing in BTC (J.S.) based on hematoxylin and eosin slides and cytokeratin expression. As a small ROI may inadvertently lead to variations in the results [21], we selected 7-16 ROIs for each subdivided region and 29-43 ROIs for each tumor tissue section. The images were analyzed using inForm 2.4.4 image analysis software (Perkin Elmer) and Spotfire software (TIBCO Software Inc., Palo Alto, CA). The counted cell numbers were expressed as the mean number of cells/mm^2 for each cell population.

Table 1. Clinical characteristics of the study patients with biliary tract cancer

Variable	Value
Age (yr)	59 (35-77)
Male sex	29 (55.8)
ECOG PS	
0	28 (53.8)
1	20 (38.5)
2	4 (7.7)
Cancer type	
EHCCA	18 (34.6)
GBCA	19 (36.5)
IHCCA	15 (28.8)
CA 19-9 (U/mL)[a)]	75.8 (0.7-33,589)
Metastasis site	
Liver metastasis	23 (44.2)
Lung metastasis	7 (13.5)
Peritoneal metastasis	9 (17.3)
Bone metastasis	1 (1.9)
Adjuvant therapy prior to GP	
Chemotherapy	7 (13.5)
CCRT	13 (25.0)

Values are presented as median (range) or number (%). CA 19-9, cancer antigen 19-9; CCRT, concurrent chemoradiation therapy; ECOG, Eastern Cooperative Oncology Group; EHCCA, extrahepatic cholangiocarcinoma; GB, gall bladder; GP, gemcitabine plus cisplatin; IHCCA, intrahepatic cholangiocarcinoma; PS, performance status. [a)]CA 19-9 values were available for 37 patients.

3. Statistical analysis

Statistical analyses were performed using Prism software ver. 6.0 (GraphPad, La Jolla, CA) or R software ver. 3.4.1 (R Foundation for Statistical Computing, Vienna, Austria). Paired values were compared using Friedman test and Dunn's multiple comparisons test. Kruskal-Wallis test was used to compare the difference among non-paired values.

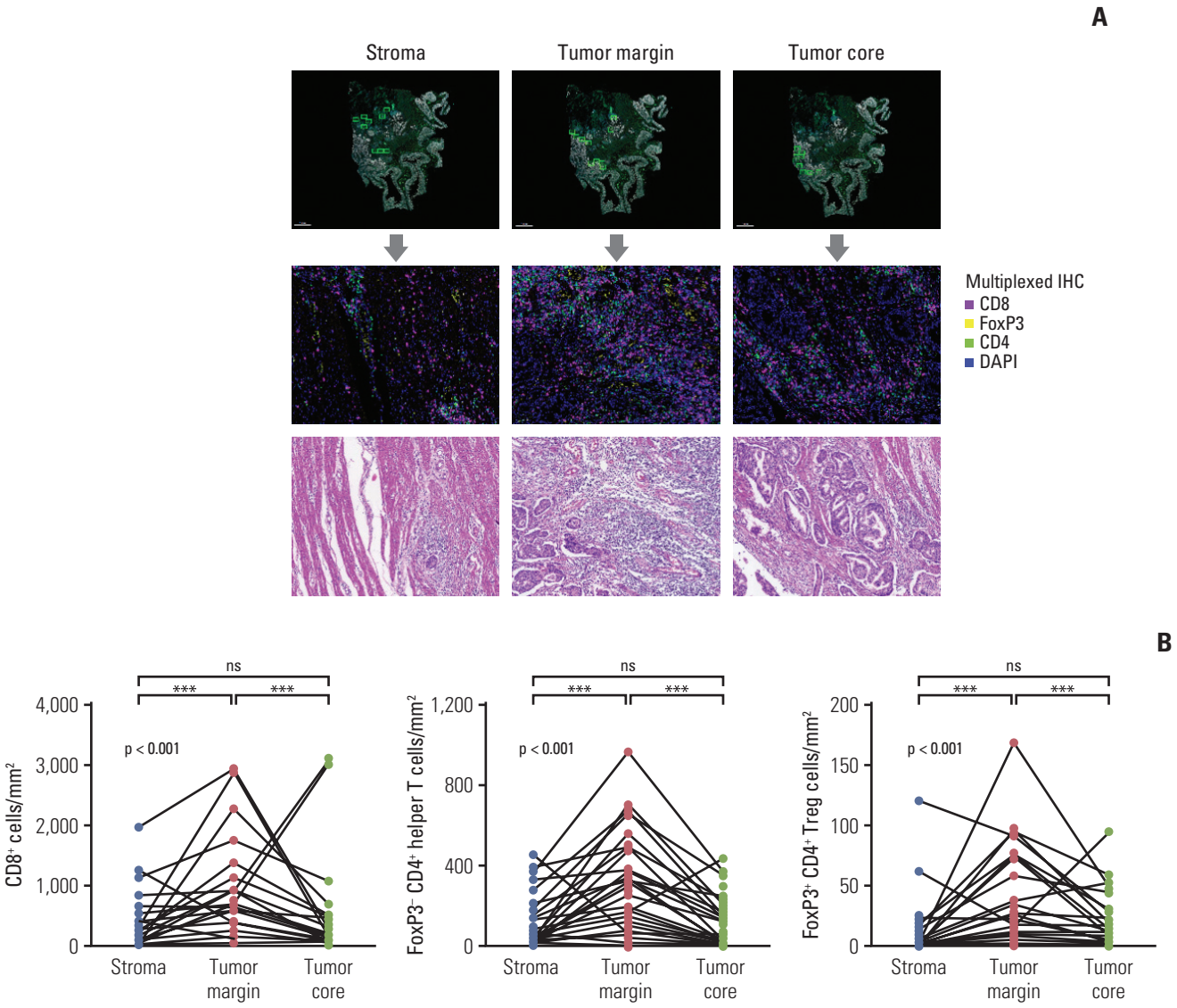

Fig. 1. Quantification of the infiltration of T cell subsets according to the spatial distribution. (A) Representative image of multiplexed immunohistochemistry (IHC) demonstrating the selection of regions of interest and fluorescence imaging. (B) Spatial distribution patterns of $CD8^+$ T cells, $FoxP3^-$ $CD4^+$ helper T cells, and $FoxP3^+$ $CD4^+$ regulatory T cells (Treg) in the tumor core, tumor margin, and stroma. ***p < 0.001; ns, not significant.

Progression-free survival (PFS) was defined as the time interval from the initiation of GemCis therapy (index date) to the date of disease progression (determined using RECIST v1.1) or death. Overall survival (OS) was defined as the time interval between the index date and date of death from any cause. The Kaplan-Meier method was used to estimate survival outcomes, and the log-rank test was used to compare these survival outcomes among the subgroups. A p-value of < 0.05 was considered significant.

Results

1. Patient characteristics

The baseline characteristics of the 52 study patients with advanced BTC are summarized in Table 1. The median age was 59 years (range, 35 to 77 years), and 55.8% of the patients were male. The Eastern Cooperative Oncology Group (ECOG) performance status was 0-1 and 2 in 48 patients (81.4%) and four patients (7.7%), respectively. The primary tumors of the study patients were as follows: EHCCA in 18 patients (34.6%), GBCA in 19 patients (36.5%), and IHCCA in

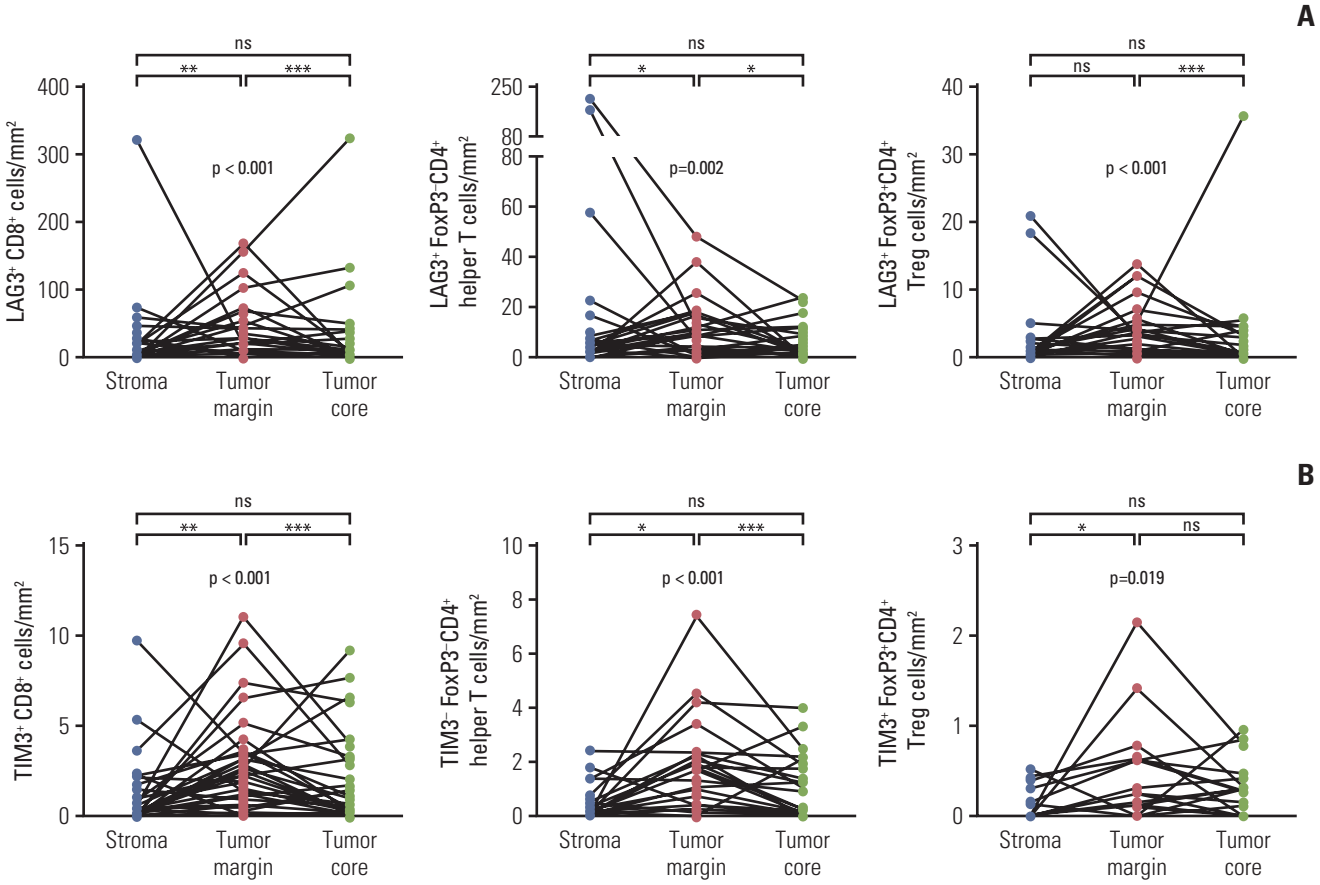

Fig. 2. Spatial distribution of LAG3- and TIM3-expressing T cell subsets. (A, B) The density of LAG3- and TIM3-expressing $CD8^+$ T cells, $FoxP3^-$ $CD4^+$ helper T cells, and $FoxP3^+$ $CD4^+$ regulatory T cells (Treg) in the tumor core, tumor margin, and stroma. *$p < 0.05$, **$p < 0.01$, ***$p < 0.001$; ns, not significant.

15 patients (28.8%). The median cancer antigen 19-9 level was 75.8 U/mL (range, 0.7 to 33,589 U/mL) at the time of the initiation of GemCis therapy. The histology was adenocarcinoma in all patients. Among the 52 study patients, 16 patients who received palliative surgery had initially stage IV disease and 36 patients had recurrence following surgery. All patients received GemCis as first-line therapy for the management of recurrent or metastatic disease. The median time from surgery to the start of GemCis was 4.72 months (95% confidence interval [CI], 3.39 to 7.27 months). The patients received a median of 5 cycles (range, 1 to 42 cycles) of GemCis. Among 14 patients with measurable disease, the best response to GemCis was partial response in four patients (28.6 %), stable disease in seven patients (50%), and progressive disease in three patients (21.4%).

Overall, the median PFS was 6.1 months (95% CI, 4.0 to 11.8 months), and the median OS was 15.2 months (95% CI, 6.6 to 31.4 months) (S2A Fig.). Survival outcomes were compared with those of the subgroups of the source population, which showed that patients in the study population had similar survival outcomes when compared with patients in the non-study group who underwent surgical resection; however, patients who did not undergo surgical resection showed inferior PFS and OS (S2B Fig.). Among the patients in this study, there was no difference in PFS and OS according to the initial disease status (initially stage IV vs. recurrent tumor) (S2C Fig.).

2. Infiltration of T cell subsets in the tumor margin

To quantify the infiltration of T cell subsets according to their spatial distribution, we first chose ROIs representing three distinct subdivided regions: stroma, tumor margin, and tumor core (Fig. 1A). The density of $CD8^+$ cytotoxic T cells, $FoxP3^-$ $CD4^+$ helper T cells, and $FoxP3^+$ $CD4^+$ regulatory T cells was significantly higher in the tumor margin than in the stroma and tumor core (Fig. 1B). The density of these T cell subset infiltrates was comparable between the stroma and tumor core (Fig. 1B). The absolute number of each

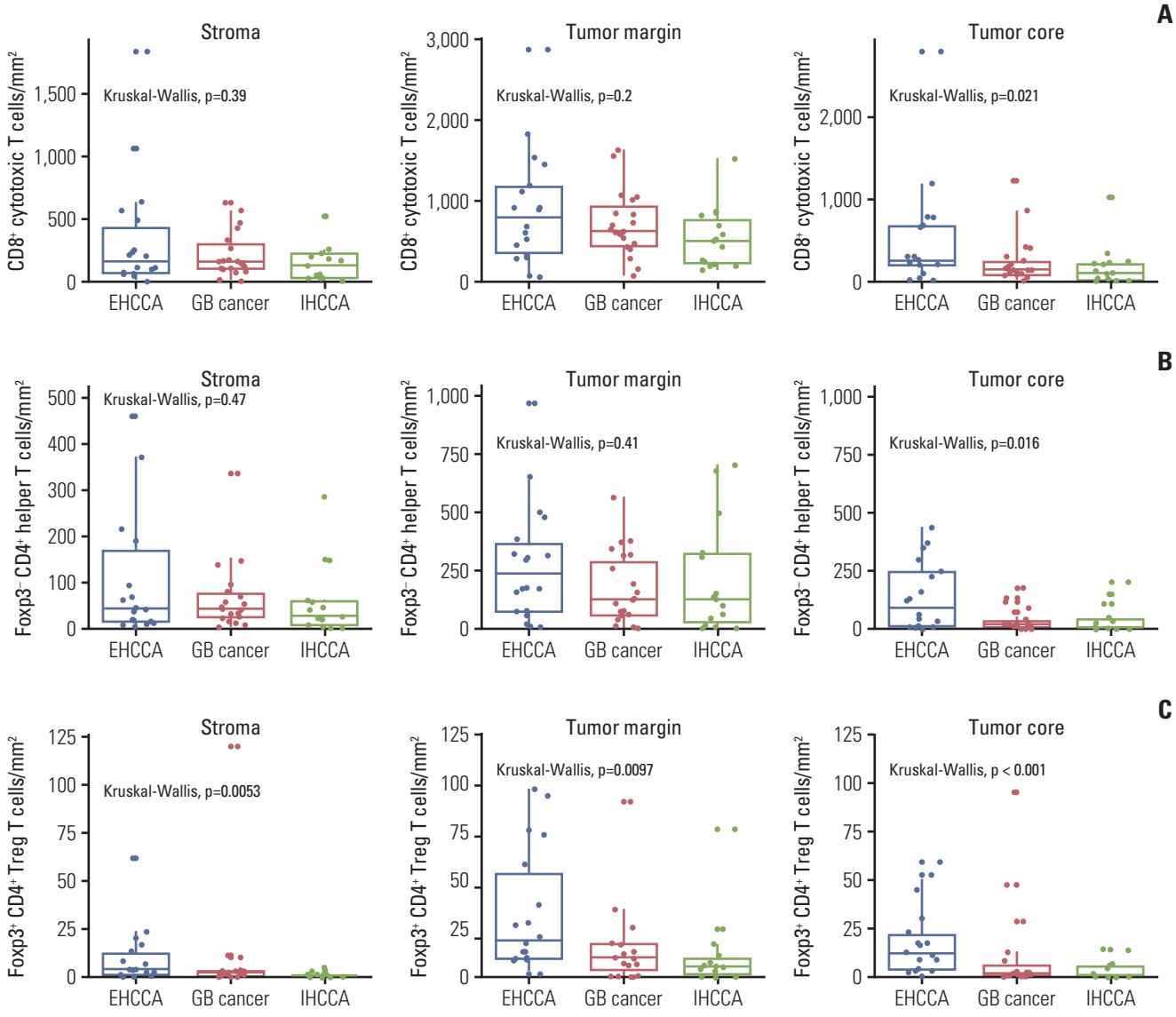

Fig. 3. Comparison of the density of T cell subset infiltrates according to the primary tumor site. (A-C) The density of $CD8^+$ T cells (A), $FoxP3^-$ $CD4^+$ helper T cells (B), and $FoxP3^+$ $CD4^+$ regulatory T cells (Treg) (C) according to the primary tumor site. EHCCA, extrahepatic cholangiocarcinoma; GB, gall bladder; IHCCA, intrahepatic cholangiocarcinoma. *$p < 0.05$, **$p < 0.01$, ***$p < 0.001$.

T cell subset per area is presented in S3 Table. The density of $FoxP3^-$ $CD4^+$ helper T cells showed a strong correlation with that of total T cells in the tumor margin and tumor core; however, the density of $FoxP3^-$ $CD4^+$ helper T cells showed a moderate but significant correlation with that of total T cells in the stroma (S4 Fig.).

The density of $CD45RO^+$ $CD8^+$ memory T cells and granzyme B^+ $CD8^+$ T cells was the highest in the tumor margin (S5 Fig.).

3. High density of TIM3- and LAG3-expressing $CD8^+$ T cells and $FoxP3^-$ $CD4^+$ helper T cells in the tumor margin

We examined T cell subsets that expressed the immune checkpoint receptors LAG3 and TIM3. The density of LAG3-expressing $CD8^+$ cytotoxic T cells and $FoxP3^-$ $CD4^+$ helper T cells was the highest in the tumor margin; however, there was no significant difference in their density between the stroma and tumor core (Fig. 2A). Likewise, the density of $LAG3^+$ $FoxP3^-$ $CD4^+$ helper T cells was higher in the tumor margin than in the stroma and tumor core (Fig. 2B). The density of $TIM3^+$ $CD8^+$ cytotoxic T cells was the highest in the

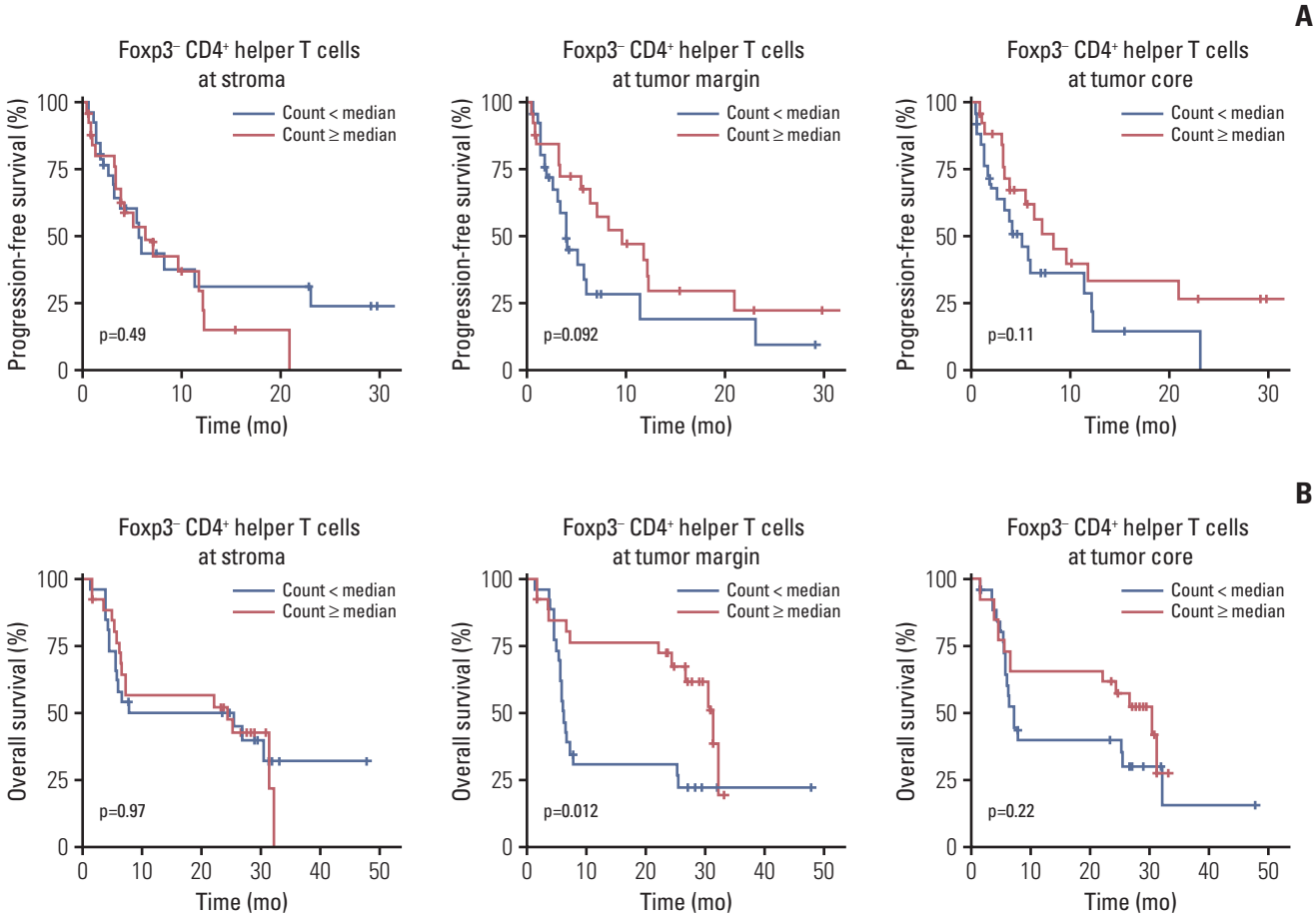

Fig. 4. Survival outcomes of biliary tract cancer patients according to the density of FoxP3⁻ CD4⁺ helper T cells. (A, B) Progression-free survival (A) and overall survival (B) of biliary tract cancer patients treated with gemcitabine plus cisplatin according to the density of FoxP3⁻ CD4⁺ helper T cells in the tumor core, tumor margin, and stroma.

tumor margin, and the tumor core exhibited a higher density of TIM3⁺ CD8⁺ infiltrates compared with the density in the stroma (Fig. 2B). Although the density of LAG3⁺ or TIM3⁺ FoxP3⁺ CD4⁺ regulatory T cells was higher in the tumor margin than in the stroma, there was no difference between the tumor margin and tumor core (Fig. 2A and B).

4. Comparison of the density of T cell subset infiltrates according to the primary tumor site

The density of CD8⁺ cytotoxic T cells in the stroma and tumor margin was comparable among EHCCA, GBCA, and IHCCA; however, the density in the tumor core was significantly higher in EHCCA than in GBCA and IHCCA (Fig. 3A). The density of FoxP3⁻ CD4⁺ helper T cells also showed no difference among the cancer types in the stroma and tumor margin; however, the density of the infiltrates in the tumor core was the highest in EHCCA (Fig. 3B). The density of FoxP3⁺ CD4⁺ regulatory T cells was higher in EHCCA regardless of the tumor site (Fig. 3C).

5. Association of the density of FoxP3⁻CD4⁺ helper T cells in the tumor margin with the survival outcomes of BTC patients treated with GemCis

Following the determination of regional differences in the density of immune infiltrates, we examined the association between the density of T cell subset infiltrates and the efficacy of GemCis. Survival outcomes did not differ according to the density of CD8⁺ cytotoxic T cell infiltrates (≥ median vs. < median) in each tumor site: PFS (p=0.230, p=0.170, and p=0.440 for stroma, tumor margin, and tumor core, respectively); OS (p=0.640, p=0.220, and p=0.460 for stroma, tumor margin, and tumor core, respectively) (S6A and S6B Fig.).

The density of FoxP3⁻ CD4⁺ helper T cells (≥ median vs. < median) in the stroma and tumor core was not associated with PFS (p=0.490 and p=0.110 for stroma and tumor core, respectively) and OS (p=0.970 and p=0.220 for stroma and

Table 2. Factors associated with progression-free survival and overall survival

Variable	Progression-free survival				Overall survival			
	Univariate		Multivariate		Univariate		Multivariate	
	HR (95% CI)	p-value	HR (95% CI)	p value	HR (95% CI)	p-value	HR (95% CI)	p value
Helper T cell density > median	0.52 (0.26-1.02)	0.058	0.35 (0.17-0.74)	0.005	0.42 (0.21-0.85)	0.016	0.34 (0.17-0.71)	0.004
Age	1.00 (0.97-1.03)	0.947	-	-	1.00 (0.97-1.04)	0.893	-	-
Male sex	0.90 (0.46-1.75)	0.749	-	-	0.83 (0.42-1.64)	0.598	-	-
Measurable disease[a)]	1.06 (0.5-2.21)	0.887	-	-	1.32 (0.63-2.76)	0.466	-	-
Initially stage IV	1.27 (0.60-2.69)	0.536	-	-	1.02 (0.50-2.11)	0.951	-	-
ECOG PS ≥ 2	3.12 (1.51-6.43)	0.002	4.25 (1.95-9.26)	< 0.001	2.40 (1.19-4.80)	0.014	2.91 (1.42-5.96)	0.004

CI, confidence interval; ECOG, Eastern Cooperative Oncology Group; HR, hazards ratio; PS, performance status; RECIST, Response Evaluation Criteria in Solid Tumors. [a)]Measurable disease by RECIST.

tumor core, respectively) (Fig. 4A and B). In contrast, a high density of FoxP3$^-$ CD4$^+$ helper T cells in the tumor margin (≥ median) showed a trend toward better PFS (p=0.092) and significantly better OS (p=0.012) (Fig. 4A and B). Multivariate analyses revealed that a higher density of FoxP3$^-$ CD4$^+$ helper T cells (> median) was independently associated with both PFS (hazards ratio [HR], 0.34; 95% CI, 0.17 to 0.74; p=0.005) and OS (HR, 0.34; 95% CI, 0.17 to 0.71; p=0.004) (Table 2). However, a comparison based on the cancer type showed that the difference in PFS and OS according to the density of FoxP3$^-$ CD4$^+$ helper T cells did not reach statistical significance (S7 Fig.).

The density of FoxP3$^+$ CD4$^+$ regulatory T cells was not associated with PFS (p=0.980, p=0.790, and p=0.520 for stroma, tumor margin, and tumor core, respectively) and OS (p=0.360, p=0.890, and p=0.600 for stroma, tumor margin, and tumor core, respectively) (S8A and S8B Fig.).

Discussion

In the current study, we showed that the tumor margin but not the stroma and tumor core is the main site for the active infiltration of T cell subsets through mIHC analysis. LAG3- and TIM3-expressing T cell subsets were also mostly observed in the tumor margin. Importantly, a higher density of FoxP3$^-$ CD4$^+$ helper T cell infiltrates in the tumor margin was independently associated with favorable PFS and OS following first-line GemCis. To the best of our knowledge, this is the first BTC study to focus on the spatial distribution of key T cell subsets and their clinical implications in a systemic chemotherapy setting.

Although the immune heterogeneity among cancer patients is well known [22-24], the heterogeneity of immune subsets according to their location remains unclear. We aimed to address this issue by sub-sectioning the tumor tissue into the stroma, tumor margin, and tumor core, which cannot be achieved by analyzing the whole tissue section. The clinical value of the spatial distribution of immune cells has been reported for other cancer types. The density of CD8$^+$ T cells in the invasive tumor margin rather than the tumor center demonstrated the best predictive capacity in predicting ant–programmed death-1 responses in melanoma patients [15]. On the other hand, a higher level of intratumoral but not peritumoral CD8$^+$ T cells in conjunction with a low level of myeloid cells was reported to be associated with favorable outcomes in melanoma patients treated with mitogen-activated protein kinase inhibitors. Taken together with our results showing the association between clinical outcomes and the localization of FoxP3$^-$ CD4$^+$ helper T cells, the findings suggest that the spatial distribution of immune cells could be an important factor associated with clinical outcomes and should be considered when evaluating the immune microenvironment.

Given that TIM3 and LAG3 are expressed on a highly activated and exhausted T cells [23], the abundance of LAG3 and TIM3 expression in the tumor margin suggests that this is the major site where the active engagement of T cells against tumor cells and resulting T cell exhaustion occur. Therefore, for the evaluation of active anti-tumor immune responses, it would be reasonable to obtain tumor tissues from the interface between the tumor and stroma and focus the pathological analysis on the invasive tumor margin.

CD8$^+$ T cells have been implicated as a key T cell subset in mounting anti-tumor responses [12,13] and ICI responses [15]. However, emerging evidence suggests that CD4$^+$ T cells may also play important roles. From a classical perspective, CD4$^+$ helper T cells are known to promote the priming of tumor-specific CD8$^+$ T cells and help elicit durable T cell responses by interacting with dendritic cells (DCs) in an MHC class II-dependent manner [10]. Recently, it has been

reported that clonally expanded tumor-infiltrating $CD4^+$ T cells can directly kill autologous tumor cells, and their function can be suppressed by regulatory $CD4^+$ T cells [25]. Another study showed that the anti-tumor $CD4^+$ T cell response against MHC class II-restricted neoantigens was critical for tumor rejection [25]. Moreover, a previous study of cholangiocarcinoma showed that the abundance of mature DCs in the invasive margin coincided with the enrichment of $CD4^+$ T cells in the peritumoral area [26]. Therefore, considering the prognostic relevance of $CD4^+$ helper T cells in the tumor margin observed in our study, we assume that the heterogeneity of the interaction between DCs and $CD4^+$ helper T cells among BTC cases may be an important factor that affects the magnitude of the anti-tumor response and ultimately survival outcomes. In addition, as cisplatin has been suggested to promote DC maturation and antigen presentation [27], it is also possible that cisplatin might have positively affected the helper T cell response in our clinical setting. This is in agreement with the findings of a previous study of non–small cell lung cancer, which suggested that the activation of preexisting tumor-specific $CD4^+$ T cells may promote an anti-tumor immune response that acts in synergy with cisplatin-based doublet chemotherapy [16]. Other mechanisms such as the induction of the immunogenic milieu enriched with helper T cell activating proinflammatory cytokines by chemotherapy [28] may also explain our findings.

$FoxP3^-$ $CD4^+$ helper T cells and $FoxP3^+$ $CD4^+$ regulatory T cells play opposite roles in anti-tumor immunity [10,11,25]; thus, our results showing an association between OS and $FoxP3^-$ $CD4^+$ helper T cells but not $FoxP3^+$ $CD4^+$ regulatory T cells suggest the need for a separate evaluation of these $CD4^+$ subsets. Considering that the difference between these $CD4^+$ subsets is not detectable by conventional IHC, our multiplexed approach enhanced the quality of the analysis. This novel quantitative multispectral imaging method has been validated to reflect conventional IHC-based immune cell evaluation [29] and is increasingly used to assess the immune profiles of the TME [30]. Its clinical usefulness deserves further investigation in future studies dealing with various immune subsets and clinical settings.

A comparison among the cancer types revealed a higher density of T cell subsets in the tumor core and regulatory T cells in the examined regions in EHCCA. This is in agreement with a previous study showing the increased infiltration of $CD8^+$ T cells in EHCCA [13]. However, given the uncertain clinical value of immune cells including regulatory T cells in our analysis, cancer type–specific immune features and their implications should be further investigated.

One of the limitations of this study is the use of surgical specimens that were not necessarily obtained just before GemCis therapy. We included patients with recurrence because there has been no report suggesting immune profiles substantially differ between primary and recurrent BTC, and the time from surgery to the start of GemCis was relatively short (median, 4.72 months). Nevertheless, the possibility that recurrent tumors may exhibit different immune profiles cannot be excluded, which may limit the interpretation of our results. In addition, the inclusion of patients who underwent surgical resection leading to reduced tumor burden may not be fully representative of the total BTC patient population treated with GemCis. Nevertheless, studies on spatial heterogeneity require sufficient tissue sections; thus, our approach of using surgical specimens may be the only appropriate method in an advanced disease setting. Moreover, among the patients included in this study, there was no difference in PFS and OS according to the initial disease status, suggesting that our survival data were at least not affected by the initial disease status. The interpretation of our results is also limited by the relatively small number of patients included in this study, which precluded statistically meaningful subgroup analyses. Validation of the clinical implications of the spatial distribution of immune subsets is necessary with independent cohorts and in the context of ICI treatment for the generalizability of our results.

In conclusion, the tumor margin is the major site for the active infiltration of T cell subsets with higher levels of LAG3 and TIM3 expression in BTC. The tumor margin should be the focus of studies evaluating the immune profiles of patients with BTC. Tumor margin-infiltrating $FoxP3^-$ $CD4^+$ helper T cells appear to be a key population associated with clinical outcomes in BTC patients. Their clinical value for BTC warrants further investigation in other therapeutic contexts.

Electronic Supplementary Material

Supplementary materials are available at Cancer Research and Treatment website (https://www.e-crt.org).

Ethical Statement

This study was approved by the Institutional Review Board (IRB No: 2018-0716) of Asan Medical Center (Seoul, Korea). Informed consent from patients was waived by the IRBs due to the retrospective nature of this study.

Author Contributions

Conceived and designed the analysis: Kim HD, Yoo C.
Collected the data: Kim HD, Kim JH, Ryu YM, Kim D, Lee S, Shin J, Hong SM, Kim KH, Jung DH, Song GW, Hwang DW, Lee JH, Song KB, Ryoo BY, Jeong JH, Kim KP, Kim SY, Yoo C.
Performed the analysis: Kim HD, Kim JH, Ryu YM, Kim SY, Yoo C.
Wrote the paper: Kim HD, Yoo C.

Conflicts of Interest

Conflicts of interest relevant to this article was not reported.

Acknowledgments

We thank the optical imaging core facility at the ConveRgence mEDIcine research cenTer (CREDIT), Asan Medical Center for support and instrumentation.

This study was funded by the grant from Asan Institute for Life Sciences, Asan Medical Center, Seoul, Korea (2017IL0752).

References

1. Valle J, Wasan H, Palmer DH, Cunningham D, Anthoney A, Maraveyas A, et al. Cisplatin plus gemcitabine versus gemcitabine for biliary tract cancer. N Engl J Med. 2010;362:1273-81.
2. Chae H, Kim D, Yoo C, Kim KP, Jeong JH, Chang HM, et al. Therapeutic relevance of targeted sequencing in management of patients with advanced biliary tract cancer: DNA damage repair gene mutations as a predictive biomarker. Eur J Cancer. 2019;120:31-9.
3. Abou-Alfa GK, Macarulla T, Javle MM, Kelley RK, Lubner SJ, Adeva J, et al. Ivosidenib in IDH1-mutant, chemotherapy-refractory cholangiocarcinoma (ClarIDHy): a multicentre, randomised, double-blind, placebo-controlled, phase 3 study. Lancet Oncol. 2020;21:796-807.
4. Abou-Alfa GK, Sahai V, Hollebecque A, Vaccaro G, Melisi D, Al-Rajabi R, et al. Pemigatinib for previously treated, locally advanced or metastatic cholangiocarcinoma: a multicentre, open-label, phase 2 study. Lancet Oncol. 2020;21:671-84.
5. Yoo C, Oh DY, Choi HJ, Kudo M, Ueno M, Kondo S, et al. Phase I study of bintrafusp alfa, a bifunctional fusion protein targeting TGF-beta and PD-L1, in patients with pretreated biliary tract cancer. J Immunother Cancer. 2020;8:e000564.
6. Ueno M, Ikeda M, Morizane C, Kobayashi S, Ohno I, Kondo S, et al. Nivolumab alone or in combination with cisplatin plus gemcitabine in Japanese patients with unresectable or recurrent biliary tract cancer: a non-randomised, multicentre, open-label, phase 1 study. Lancet Gastroenterol Hepatol. 2019;4:611-21.
7. Piha-Paul SA, Oh DY, Ueno M, Malka D, Chung HC, Nagrial A, et al. Efficacy and safety of pembrolizumab for the treatment of advanced biliary cancer: results from the KEYNOTE-158 and KEYNOTE-028 studies. Int J Cancer. 2020;147:2190-8.
8. Kang J, Jeong JH, Hwang HS, Lee SS, Park DH, Oh DW, et al. Efficacy and safety of pembrolizumab in patients with refractory advanced biliary tract cancer: tumor proportion score as a potential biomarker for response. Cancer Res Treat. 2020;52:594-603.
9. Waldman AD, Fritz JM, Lenardo MJ. A guide to cancer immunotherapy: from T cell basic science to clinical practice. Nat Rev Immunol. 2020;20:651-68.
10. Borst J, Ahrends T, Babala N, Melief CJ, Kastenmuller W. CD4(+) T cell help in cancer immunology and immunotherapy. Nat Rev Immunol. 2018;18:635-47.
11. Togashi Y, Shitara K, Nishikawa H. Regulatory T cells in cancer immunosuppression: implications for anticancer therapy. Nat Rev Clin Oncol. 2019;16:356-71.
12. Kitano Y, Okabe H, Yamashita YI, Nakagawa S, Saito Y, Umezaki N, et al. Tumour-infiltrating inflammatory and immune cells in patients with extrahepatic cholangiocarcinoma. Br J Cancer. 2018;118:171-80.
13. Goeppert B, Frauenschuh L, Zucknick M, Stenzinger A, Andrulis M, Klauschen F, et al. Prognostic impact of tumour-infiltrating immune cells on biliary tract cancer. Br J Cancer. 2013;109:2665-74.
14. Massi D, Rulli E, Cossa M, Valeri B, Rodolfo M, Merelli B, et al. The density and spatial tissue distribution of CD8(+) and CD163(+) immune cells predict response and outcome in melanoma patients receiving MAPK inhibitors. J Immunother Cancer. 2019;7:308.
15. Tumeh PC, Harview CL, Yearley JH, Shintaku IP, Taylor EJ, Robert L, et al. PD-1 blockade induces responses by inhibiting adaptive immune resistance. Nature. 2014;515:568-71.
16. Godet Y, Fabre E, Dosset M, Lamuraglia M, Levionnois E, Ravel P, et al. Analysis of spontaneous tumor-specific CD4 T-cell immunity in lung cancer using promiscuous HLA-DR telomerase-derived epitopes: potential synergistic effect with chemotherapy response. Clin Cancer Res. 2012;18:2943-53.
17. Yuan Y. Spatial heterogeneity in the tumor microenvironment. Cold Spring Harb Perspect Med. 2016;6:a026583.
18. Heindl A, Nawaz S, Yuan Y. Mapping spatial heterogeneity in the tumor microenvironment: a new era for digital pathology. Lab Invest. 2015;95:377-84.
19. Kather JN, Suarez-Carmona M, Charoentong P, Weis CA, Hirsch D, Bankhead P, et al. Topography of cancer-associated immune cells in human solid tumors. Elife. 2018;7:e36967.
20. Kim BJ, Hyung J, Yoo C, Kim KP, Park SJ, Lee SS, et al. Prognostic factors in patients with advanced biliary tract cancer treated with first-line gemcitabine plus cisplatin: retrospective analysis of 740 patients. Cancer Chemother Pharmacol. 2017;80:209-15.
21. Christgen M, von Ahsen S, Christgen H, Langer F, Kreipe H. The region-of-interest size impacts on Ki67 quantification by computer-assisted image analysis in breast cancer. Hum Pathol. 2015;46:1341-9.
22. Thorsson V, Gibbs DL, Brown SD, Wolf D, Bortone DS, Ou Yang TH, et al. The immune landscape of cancer. Immunity. 2018;48:812-30.
23. Kim HD, Song GW, Park S, Jung MK, Kim MH, Kang HJ, et al. Association between expression level of PD1 by tumor-infiltrating CD8(+) T cells and features of hepatocellular carcinoma. Gastroenterology. 2018;155:1936-50.

24. Kim HD, Park S, Jeong S, Lee YJ, Lee H, Kim CG, et al. 4-1BB delineates distinct activation status of exhausted tumor-infiltrating CD8(+) T cells in hepatocellular carcinoma. Hepatology. 2020;71:955-71.
25. Oh DY, Kwek SS, Raju SS, Li T, McCarthy E, Chow E, et al. Intratumoral CD4(+) T cells mediate anti-tumor cytotoxicity in human bladder cancer. Cell. 2020;181:1612-25.
26. Takagi S, Miyagawa S, Ichikawa E, Soeda J, Miwa S, Miyagawa Y, et al. Dendritic cells, T-cell infiltration, and Grp94 expression in cholangiocellular carcinoma. Hum Pathol. 2004;35:881-6.
27. Jackaman C, Majewski D, Fox SA, Nowak AK, Nelson DJ. Chemotherapy broadens the range of tumor antigens seen by cytotoxic CD8(+) T cells in vivo. Cancer Immunol Immunother. 2012;61:2343-56.
28. Ding ZC, Zhou G. Cytotoxic chemotherapy and CD4+ effector T cells: an emerging alliance for durable antitumor effects. Clin Dev Immunol. 2012;2012:890178.
29. Soh JS, Jo SI, Lee H, Do EJ, Hwang SW, Park SH, et al. Immunoprofiling of colitis-associated and sporadic colorectal cancer and its clinical significance. Sci Rep. 2019;9:6833.
30. Hofman P, Badoual C, Henderson F, Berland L, Hamila M, Long-Mira E, et al. Multiplexed immunohistochemistry for molecular and immune profiling in lung cancer-just about ready for prime-time? Cancers (Basel). 2019;11:283.